

Article

Dynamic Health Monitoring of Aero-Engine Gas-Path System Based on SFA-GMM-BID

Dewen Li ¹, Yang Li ¹, Tianci Zhang ^{1,2}, Jing Cai ², Hongfu Zuo ² and Ying Zhang ^{1,2,*}¹ College of Automobile and Traffic Engineering, Nanjing Forestry University, Nanjing 210037, China² School of Civil Aviation, Nanjing University of Aeronautics and Astronautics, Nanjing 210016, China

* Correspondence: zhangyingrms@njfu.edu.cn; Tel.: +86-181-0061-1200

Abstract: This paper proposes a dynamic health monitoring method for aero-engines by extracting more hidden information from the raw values of gas-path parameters based on slow feature analysis (SFA) and the Gaussian mixture model (GMM) to improve the capability of detecting gas-path faults of aero-engines. First, an SFA algorithm is used to process the raw values of gas-path parameters, extracting the effective features reflecting the slow variation of the gas-path state. Then, a GMM is established based on the slow features of the target aero-engine in a normal state to measure its health status. Moreover, an indicator based on the Bayesian inference distance (BID) is constructed to quantitatively characterize the performance degradation degree of the target aero-engine. Considering that the fixed threshold does not suit the time-varying characteristics of the gas-path state, a dynamic threshold based on the maximum information coefficient is designed for aero-engine health monitoring. The proposed method is verified using a set of actual operation data of a certain aero-engine. The results show that the proposed method can better reflect the degradation process of the aero-engine and identify aero-engine anomalies earlier than other aero-engine fault detection methods. In addition, the dynamic threshold can reduce the occurrence of false alarms. All these advantages give the proposed method high value in real-world applications.

Keywords: aero-engine; slow feature analysis; Gaussian mixture model; Bayesian inference distance; dynamic threshold



Citation: Li, D.; Li, Y.; Zhang, T.; Cai, J.; Zuo, H.; Zhang, Y. Dynamic Health Monitoring of Aero-Engine Gas-Path System Based on SFA-GMM-BID.

Electronics **2023**, *12*, 3199. <https://doi.org/10.3390/electronics12143199>

Received: 20 June 2023

Revised: 16 July 2023

Accepted: 23 July 2023

Published: 24 July 2023



Copyright: © 2023 by the authors. Licensee MDPI, Basel, Switzerland. This article is an open access article distributed under the terms and conditions of the Creative Commons Attribution (CC BY) license (<https://creativecommons.org/licenses/by/4.0/>).

1. Introduction

In recent years, with the rapid development of intelligent manufacturing and the industrial Internet, health monitoring has been widely used in vehicle control systems [1,2], battery health management systems [3–5], operation and maintenance systems of key components of equipment [6–8], and other engineering systems. As aero-engines operate in harsh working conditions (high temperature, high load, etc.) repeatedly, the performance of each aero-engine will degrade gradually from the time it is put into use, and such performance degradation will increase the risk of aircraft accidents [9–11]. Therefore, strengthening the health monitoring of aero-engines and improving flight safety is a key concern for the aviation industry and a hot topic in civil aviation. The gas-path system is the core of an aero-engine. Research shows that gas-path faults cause more than 90% of aero-engine failures, and the repair and maintenance cost of the gas-path system accounts for about 60% of an aero-engine's total repair and maintenance cost [12]. The capability of detecting anomalies in the aero-engine in time is essential for the health monitoring of the engine gas-path system. If anomalies in the aero-engine can be detected early, the maintenance team will have enough time to make a sound maintenance plan [13–16].

Researchers have conducted extensive research on the health monitoring of engine gas paths. The existing health monitoring methods for aero-engine gas paths can be classified into two categories: model-based gas-path health monitoring and data-driven gas-path health monitoring methods. Model-based gas-path health monitoring methods require

establishing an accurate physical–mathematical model of the engine to describe its working characteristics [17,18]. However, since an aero-engine is a piece of large and complex equipment, the lack of prior knowledge often makes it impossible to establish an accurate mathematical model. Moreover, the aero-engine is susceptible to the influence of the external environment and flight conditions in the actual operation process, so it is difficult for the established model to meet the practical needs. Contrary to the model-based gas-path health monitoring methods, the data-driven methods fully use the actual data of the aircraft in operation and extract useful hidden information to characterize the normal and abnormal states. Therefore, these methods have good generalization ability and adaptability. For this reason, data-driven gas-path health monitoring methods have been extensively studied and widely used. Smart E et al. [19] and Melnyk I et al. [20] perform anomaly monitoring of aeroengines by building two-term classifiers and autoregressive models, respectively. X. Zhou et al. [11] used a residual back-propagation neural network to mine the deviation values of gas-path parameters and combined this method with a support vector machine to achieve aero-engine health monitoring. The above data-driven gas-path health monitoring methods have achieved positive results, but their usefulness is still limited by many deficiencies, including the need for a large number of training samples, the use of highly complex models, and the susceptibility to the influence of high-dimensional data with complex correlations. With the development of comprehensive data processing technology and new cross-discipline fields, developing gas-path health monitoring methods based on information fusion has gradually become a research hotspot in the subfield of data-driven gas-path health monitoring in recent years. According to the type of input information, the gas-path health monitoring method based on information fusion can be divided into three levels: data-level fusion, feature-level fusion, and decision-level fusion. Different from the other two categories, feature-level fusion achieves considerable information compression; the extracted features reflect the information related to the actual health condition, and the fusion results fully reflect the state changes of the engine. W. Jiang [21] devised a method combining an integrated autoencoder with a self-organizing mapping neural network to fuse features, achieving good results in characterizing the operation status of the aero-engine. H. Wang [22] established a fault detection model based on the fusion of multi-parameter information of the engine achieved using the isolated forest method. The authors also verified the model's effectiveness by injecting different faults. The above methods can achieve good performance in the health monitoring of aero-engines.

Data-driven aero-engine health monitoring relies on gas-path data. However, the raw values of gas-path parameters have high dimensionality and contain too much noise and complex correlations, so these raw values need to go through dimension reduction or feature extraction treatment before they can be used in aero-engine health monitoring. For the processing of the original values of gas-channel parameters, the feature extraction method based on dimension reduction can reduce the data dimension and sort out the existing data. For instance, F. Lu et al. [23] proposed an iterative reduced-dimension kernel principal component analysis (IRKPCA) algorithm for extracting the fault features from high-dimensional data of the aero-engine. However, extracting features in high-dimensional space may bring undesired consequences, such as fusing irrelevant features and insufficient distinguishing of features. Deep learning is often used in feature extraction, which can not only learn the intrinsic laws of sample data, but also significantly improve the efficiency and effect of the algorithm [11,24]. Deep learning can be employed to learn the hidden pattern in sample data, but such feature extraction methods have poor interpretability (because the model is a black box) and need a large number of samples for model training (which is time-consuming). The degradation of aero-engine gas-path components caused by impairment accumulation and structural deformation is a slow time-varying process. Slow feature analysis (SFA) has been proposed to find a set of input and output functions that can make the output signal change as slowly as possible. It is a method to learn the salient features of time series. The extracted slow features can capture the trend of process changes and accurately distinguish the normal process

changes from the real dynamic anomalies. SFA is often used in monitoring industrial processes. H. Wang [25] used SFA to extract data features from dynamic industrial process data and combined this method with Gaussian process regression to establish a dynamic performance evaluation model. C. Cheng et al. [26] used the Hellinger distance to improve SFA and applied it to the early fault diagnosis of high-speed trains, achieving good results.

Aero-engines are highly nonlinear and time-varying in the operation process, so identifying the anomalies of the engine in time and effectively is essential for the health monitoring of the engine gas path, and it is necessary to reduce the false alarms as much as possible while ensuring a high detection rate. A fixed threshold does not suit the time-varying characteristics of the gas-path state, so it is necessary to dynamically adjust the threshold throughout the whole service life of the aero-engine [27,28]. Aiming at the time-varying characteristics of complex operating states, some scholars [29,30] proposed a threshold setting method based on the sliding window model. The traditional sliding window model directly abandons historical data or adopts some weighted forgetting factor to reduce the influence of historical data. Therefore, the choice of historical data is subject to the empirical limitation. To solve this problem, J. Shi [31] and B. Song [32] et al. used the mean square value or mutual information of the data, respectively, in different sliding windows to adjust the forgetting factor in real time, which improved the adaptive ability and update efficiency of the threshold.

In this study, we established a Gaussian mixture model (GMM) based on the Bayesian inference distance (BID) for evaluating the degradation degree of the gas path of an aero-engine based on the effective features extracted by SFA and devised a method of monitoring the health of the engine gas path based on the dynamic threshold. The main contributions of this study are as follows:

- (1) This paper takes the complete aircraft operation data obtained from the China Academy of Civil Aviation Science and Technology as the research object. The problems of unreal simulation data and incomplete experimental data of the aeroengine can be solved.
- (2) An SFA algorithm is used to extract the time-varying slow features from the raw values of gas-path parameters. These features can reflect the characteristics of gas-path changes and, therefore, can be used to achieve health monitoring of aero-engine gas paths.
- (3) This paper proposes a GMM based on BID, which uses multiple features to characterize the degradation degree of the target aero-engine. The proposed method has better applicability compared with other evaluation methods.
- (4) A dynamic threshold mechanism based on the maximum information coefficient is designed for aero-engine health monitoring to suit the time-varying characteristics of the gas-path state, which improves the sensitivity of health monitoring and effectively reduces the occurrence of false alarms.

The remainder of this paper is organized as follows: Section 2 briefly describes the composition and monitoring data of the aero-engine used as the research object in this study. Section 3 describes the theoretical basis of this study. Section 4 describes the dynamic aero-engine health monitoring method based on SFA and GMM-BID. Section 5 discusses the experimental results. In Section 6, the accuracy of the proposed method is verified through comparison. Section 7 is the conclusion.

2. Dataset and Parameter Selection

2.1. Abnormal Case Introduction

In the practical engineering application of aero-engine anomaly monitoring, the EGT value will increase when the engine performance deteriorates, and when EGT exceeds the factory-set threshold, the engine hot end components will be damaged. Therefore, the EGT of aeroengines needs to be closely monitored to prevent it from exceeding the limit value. The experimental data selected in this paper are from the left engine EGT overtemperature event found. Case 1 data are the flight data of a B737 aircraft engine from 18 May 2019 to 19 May 2020, with a total of 958 flights, defined as 958 cycles. Case 2 data are the flight

data of a B737 aircraft engine from 7 February 2020 to 20 August 2020, a total of 319 flights, defined as 319 cycles.

2.2. Parameter Selection

The research object of this paper is the CFM56_7B engine used in the B737 provided by the China Academy of Civil Aviation Science and Technology, which is a typical dual-rotor turbofan aero-engine. The engine contains six gas-path components, which are (in the order from the inlet to the outlet of the engine): fan, low-pressure compressor (LPC), high-pressure compressor (HPC), combustor, high-pressure turbine (HPT), and low-pressure turbine (LPT). Figure 1 illustrates the composition and the key gas-path monitoring parameters of a typical dual-rotor aero-engine [33].

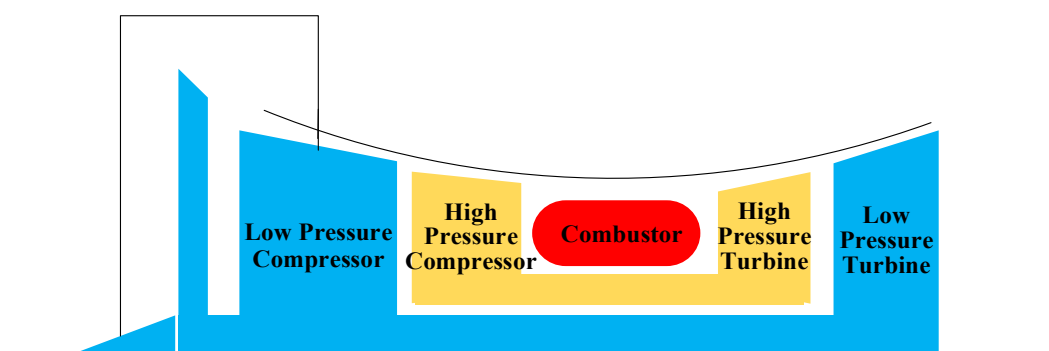


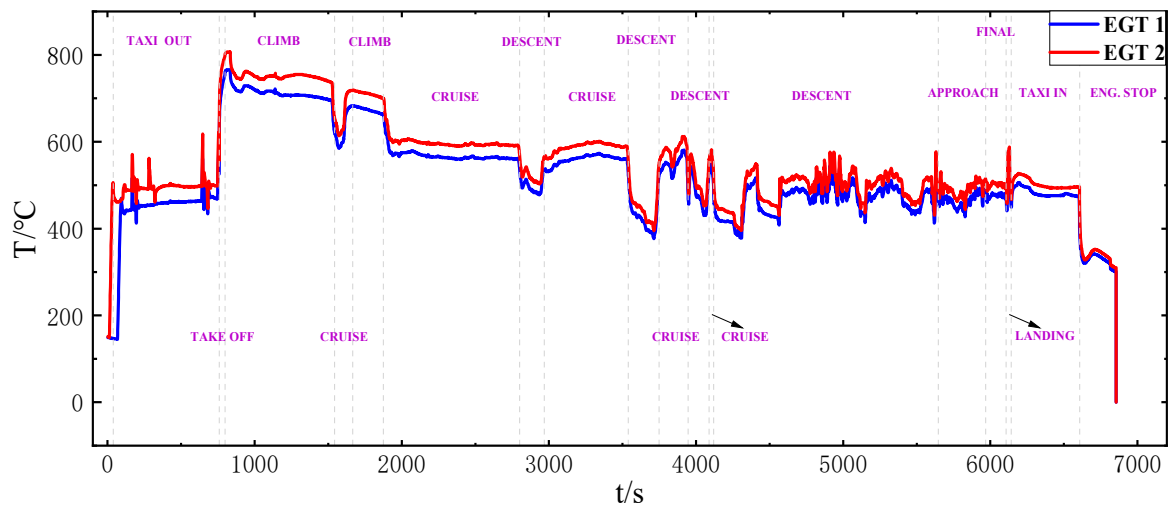
Figure 1. Composition and key gas-path monitoring parameters of a typical dual-rotor aero-engine.

An array of sensors are installed at different locations along the air path and other positions of the aviation engine to facilitate operation state monitoring and state control, and the acquired data are recorded in the Quick Access Recorder (QAR). The dataset used in this study is composed of data pieces selected from the repository of QAR data of B737 aircraft engines owned by a certain airline. The QAR monitoring parameters are a comprehensive set of measured and recorded parameters with high sampling frequency during the flight. These parameters are sensitive to intermittent anomalies of aero-engines. QAR data encompass a large number of performance parameters, but not all of them are suitable for engine health assessment. Considering that some parameters have nothing to do with the health status of the engine, and the recorded data of some parameters are incomplete, it is necessary to select the parameters that have complete records and are closely related to the health status of the engine for evaluating the health of the engine [34]. In the process of engine monitoring conducted by airlines, the exhaust gas temperature (EGT), fuel flow (FF), low-pressure rotor speed (N1), and high-pressure rotor speed (N2) are commonly used monitoring parameters. Based on the experience of engineers and the completeness of the data of each parameter in the QAR data repository, we selected six parameters, namely, exhaust gas temperature (EGT), fuel flow (FF), low-pressure rotor speed (N1), high-pressure rotor speed (N2), total outlet temperature of the low-pressure compressor (T25), and total outlet temperature of the high-pressure compressor (T3), for evaluating the health of the aero-engine. The sampling frequency of each parameter is 1 Hz. These parameters are listed in Table 1.

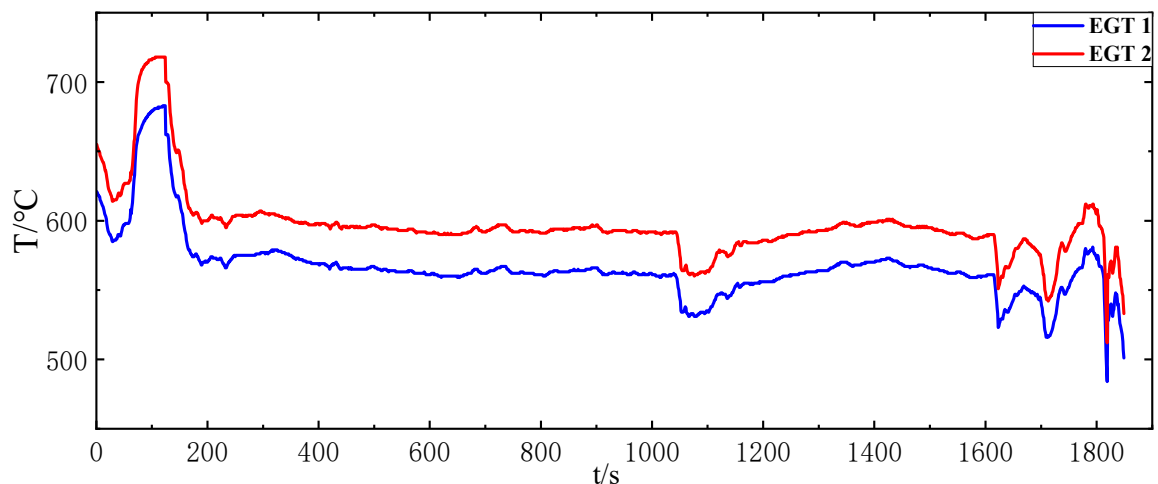
During a flight, the airplane usually goes through the following states: stationed, sliding out, taking off, climbing, cruising, approaching, and sliding in. Figure 2 shows the variation of EGT of a certain aero-engine during a flight on 20 March 2019. In the figure, EGT 1 represents the EGT monitoring data of the left aero-engine, while EGT 2 represents the EGT monitoring data of the right aero-engine.

Table 1. The selected six aero-engine performance parameters.

Symbol	Description	Unit
EGT	Exhaust gas temperature	°C
FF	Fuel flow	Lb/h
N1	Low-pressure rotor speed	rpm
N2	High-pressure rotor speed	rpm
T25	Total temperature at LPC outlet	°C
T3	Total temperature at HPC outlet	°C

**Figure 2.** EGT monitoring data of an aero-engine recorded in the process of a flight.

Considering that the monitoring data of the aero-engine exhibits different characteristics in different flight stages and that the data variation trend in the cruise stage is relatively stable, we selected the aero-engine data acquired in the cruise stage for health monitoring. The variation of EGT in the cruise stage is shown in Figure 3.

**Figure 3.** Variation of EGT of an aero-engine in the cruise stage.

3. Theoretical Basis

In this study, we established a Gaussian mixture model (GMM) based on the Bayesian inference distance (BID) for evaluating the degradation degree of the gas path of an aero-engine based on the effective features extracted by SFA and devised a method of monitoring the health of the engine gas path based on the dynamic threshold. Therefore, this section includes three parts: the feature extraction method based on Slow Feature Analysis (SFA),

the construction of the Gaussian mixture model based on the Bayesian inference distance, and the dynamic threshold design based on the maximum information coefficient.

3.1. SFA-Based Feature Extraction Approach

Slow feature analysis (SFA) has been proposed to find a set of input and output functions that can make the output signal change as slowly as possible [35]. The degradation of aero-engine gas-path components caused by impairment accumulation and structural deformation is a slow time-varying process. Based on the six aeroengine airpath performance parameter datasets selected in Part 2, slow feature analysis will be used to capture the trend of process changes of the gas-path system, and then generate features as the inputs of the Gaussian mixture model. The process of SFA-based feature extraction approach is as follows.

3.1.1. Mathematical Description of SFA

Given an n-dimensional input signal $x = [x_1, x_2, \dots, x_n]^T$, considering a linear mapping function, we can find the mapping relationship between the objective function and the input function through SFA [26]:

$$s_j = g_j = w_j^T x \tag{1}$$

where w_j^T represents the weight of the j-th function.

Accordingly, the objective function of the SFA mapping function is

$$\min \Delta(s_j(t)) = \min \langle \dot{s}_j^2 \rangle_t = \min w_j^T \langle \dot{x}_j^T \dot{x}_j \rangle_t w_j \tag{2}$$

where $\Delta(\bullet)$ represents the difference value, \dot{s} represents the time difference of s, and $\langle s \rangle_t$ is the average value of s along the time axis.

In addition, the optimization of the objective function should meet the following conditions:

$$\langle s_j \rangle_t = w_j^T x_j = 0 \tag{3}$$

$$\langle s_j^2 \rangle_t = w_j^T \langle x_j^T x_j \rangle_t w_j = 1 \tag{4}$$

$$\forall i \neq j, \langle s_i s_j \rangle_t = 0 \tag{5}$$

Finally, this problem can be transformed into the problem of decomposing generalized eigenvalue:

$$AW = BW\Omega \tag{6}$$

where $A = \langle \dot{x}^T \dot{x} \rangle_t$, $W = [w_1, w_2 \dots w_n]$, $B = \langle x^T x \rangle_t$, and Ω is the diagonal matrix of generalized eigenvalues.

3.1.2. Solution of the SFA Model

The procedure for solving the above optimization problem is as follows:

Firstly, matrix B undergoes singular value decomposition, whitening the data to eliminate correlation.

$$B = x^T x = U\Lambda U^T \tag{7}$$

Based on the above equation, the operation of data whitening can be expressed as:

$$z = \Lambda^{-\frac{1}{2}} U^T x \tag{8}$$

where the whitening matrix is $Q = \Lambda^{-\frac{1}{2}} U$, and the whitening data z satisfy $\langle z \rangle_t = Q^T \langle x \rangle_t = 0$, $\langle z^T z \rangle_t = Q \langle x^T x \rangle_t Q^T = I$.

Finding the solution through SFA can be expressed as:

$$s_j = w_j^T x = W(Q^T)^{-1} z = Pz \quad (9)$$

Therefore, the optimization problem is equivalent to solving the matrix P to minimize the whitening matrix Q. Singular value decomposition is performed on $\langle \dot{z}^T \dot{z} \rangle_t$ to attain $\langle \dot{z}^T \dot{z} \rangle_t = P\Omega P^T$, then the transformation matrix W can be calculated:

$$W = P\Lambda^{-\frac{1}{2}}U^T \quad (10)$$

After the transformation matrix W is obtained, the slow feature s can be expressed as

$$s = Pz = Wx \quad (11)$$

3.2. Gaussian Mixture Model (GMM)

In order to quantitatively characterize the performance degradation degree of the aero-engine air-path system, it is necessary to establish an appropriate health index. GMM is a model based on multiple Gaussian probability density functions (normal distribution curves) [36]. Data with complex distributions during aero-engine operation can be well described when only healthy-state data are available. Therefore, we established a Gaussian mixture model (GMM) based on the Bayesian inference distance (BID) for evaluating the degradation degree of the gas path of an aero-engine based on the effective features extracted by SFA.

GMM uses the expectation maximization (EM) algorithm [37] to train the Gaussian distribution model, which is expressed as:

$$p(x) = \sum_{m=1}^M \pi_m p(x|\theta_m) \quad (12)$$

where M is the number of single Gaussian models in the model; π_m is the weight coefficient of the single Gaussian models in the mixed model, and $\sum \pi_m = 1$; $p(x|\theta_m)$ is the m -th Gaussian distribution function—its mean value is μ_m , and its covariance matrix is S_m . Denote $\phi = \{\pi_1, \dots, \pi_m; \mu_1, \dots, \mu_m; S_1, \dots, S_m\}$, the formula is:

$$p(x|\phi) = \sum_{m=1}^M \pi_m p(x|\theta_m) \quad (13)$$

Based on the above modeling, the next step is establishing a health status baseline GMM model based on healthy-state data. Traditional GMM models the negative log likelihood probability (NLLP) to evaluate health status [38]. In this paper, a quantitative indicator based on BID [39] is used as the fusion index to quantitatively evaluate the health status of the aero-engine.

Given K Gaussian classification types, among which C_k is the k -th component, the occurrence probability of each component is denoted as α_k , and the probability of the test point x_t belonging to the k -th component C_k is denoted as $p(C_k|x_t)$.

$$p(C_k|x_t) = \frac{\alpha_k p(x_t|C_k)}{p(x_t)} = \frac{\alpha_k p(x_t|C_k)}{\sum_{i=1}^K \alpha_i p(x_t|C_i)} \quad (14)$$

where α_k is the prior probability, which is obtained from the modeling data. The parameter $p(x_t|C_k)$ can be expressed as:

$$p(x_t|C_k) = \frac{1}{(2\pi)^{\frac{1}{2}}|S_k|^{\frac{1}{2}}} \exp\left[-\frac{1}{2}(x_t - \mu_k)^T S_k^{-1}(x_t - \mu_k)\right] \tag{15}$$

where the mean value of the k -th Gaussian component is μ_k , and the covariance matrix is S_k . The distance from x_t to each component C_k can be expressed as:

$$D_{C_k}(x_t) = (x_t - \mu_k)^T S_k^{-1}(x_t - \mu_k) \tag{16}$$

The value of BID is the weighted sum of the distances of all components of a single test point, which can be expressed as:

$$BID = \sum_{k=1}^K p(C_k|x_t)D_{C_k}(x_t) \tag{17}$$

3.3. Recursive Updating of Statistical Control Limits

For health monitoring of the engine, it is necessary to threshold the constructed HI to trigger an early warning. In order to adapt to the high nonlinearity and time-varying during the operation of the aero-engine, dynamically adjusting the threshold throughout the whole service life of the aero-engine is needed. In this study, a sliding window model based on the maximum information coefficient is proposed to dynamically update the threshold to reduce false alarms.

3.3.1. Sliding Window Model

It is defined that all sequentially arranged data blocks of BID constitute a sliding window model [32], and the k -th data window is represented as:

$$\mathbf{X}_k = [\mathbf{x}_{k+1}, \mathbf{x}_{k+2}, \dots, \mathbf{x}_{k+L}]^T \tag{18}$$

where L is the size of the window.

After the window slides, the $(k + 1)$ -th data window is:

$$\mathbf{X}_{k+1} = [\mathbf{x}_{k+L-l}, \dots, \mathbf{x}_{k+L+H}]^T \tag{19}$$

where H is the sliding step, and l is the volume of adaptively discarded data.

3.3.2. Adaptive Selection of Sliding Window Size Based on Maximum Information Coefficient

The k -th data window is denoted as \mathbf{X}_k , the newly added data window is denoted as \mathbf{X}_H , and $I(\mathbf{X}_k, \mathbf{X}_H)$ is used to represent the mutual information between two variables. The marginal probability of the variable \mathbf{X}_k is denoted as $p(\mathbf{X}_k)$, the marginal probability of the variable \mathbf{X}_H is denoted as $p(\mathbf{X}_H)$, and $p(\mathbf{X}_k, \mathbf{X}_H)$ is used to represent the joint distribution probability of \mathbf{X}_k and \mathbf{X}_H , then the formula for calculating $I(\mathbf{X}_k, \mathbf{X}_H)$ can be expressed as:

$$I(\mathbf{X}_k, \mathbf{X}_H) = - \iint_{\mathbf{X}_H \mathbf{X}_k} p(\mathbf{X}_k, \mathbf{X}_H) \log \frac{p(\mathbf{X}_k, \mathbf{X}_H)}{p(\mathbf{X}_k)p(\mathbf{X}_H)} d\mathbf{X}_k d\mathbf{X}_H \tag{20}$$

For the two data windows \mathbf{X}_k and \mathbf{X}_H , we can draw grid lines in the scatter diagram of the two variables and then divide the datasets of the two random variables. The grid $\mathbf{X}_k \times \mathbf{X}_H$ is represented by $G(X, Y)$, p_0, \dots, p_{X_k} are the coordinates of the dividing points on the abscissa axis, and q_0, \dots, q_{X_H} are the coordinates of the dividing points on the ordinate axis. Different grids $G(X, Y)$ can be obtained by changing p_1, \dots, p_{X_k-1} and q_1, \dots, q_{X_H-1} .

The maximum mutual information value among different grids $G(X, Y)$ is denoted as $\max I\{X_k, X_H\}$ [40]. Then, the value of the characteristic matrix of this segmentation mode is:

$$M_{X_k, X_H} = \frac{\max I\{X_k, X_H\}}{\log \min(X_k, X_H)} \tag{21}$$

The maximum correlation coefficient is:

$$MIC = \max\{M_{X_k, X_H}\} \tag{22}$$

With MIC serving as the forgetting factor of the old window, the old data pieces are adaptively discarded, and the forgetting number is $l = MIC \bullet L$.

3.3.3. Setting of Statistical Quantity Control Limit

According to the experience of experts in the aviation field, the occurrence frequency of outliers is high, but the outliers only exceed the normal range slightly. Therefore, the definition of outliers is simplified in this study: A value is called an outlier if:

- (a) it exceeds the normal range by m times in a period t ;
- (b) the total number of times of range exceeding is more than n .

The old data in the k -th sliding window are denoted as X_k , and its range is $[X_{\max}, X_{\min}]$, where $X_{\max} = \max\{X_k\}$, $X_{\min} = \min\{X_k\}$. Then, the control limit of the $(k+1)$ -th BID is:

$$(BID - threshold)_{k+1} = X_{\max} + m \bullet (X_{\max} - X_{\min}) / 2 \tag{23}$$

where m is the magnification factor. The number of determined abnormal values is usually less than 10. In this study, the value of m was determined as two based on the results of multiple experimental runs.

4. Aero-Engine Dynamic Health Monitoring Model Based on SFA-GMM-BID

Based on the above analysis, we devised an aero-engine health monitoring method based on the fusion of multiple features. The flowchart of the monitoring process is shown in Figure 4.

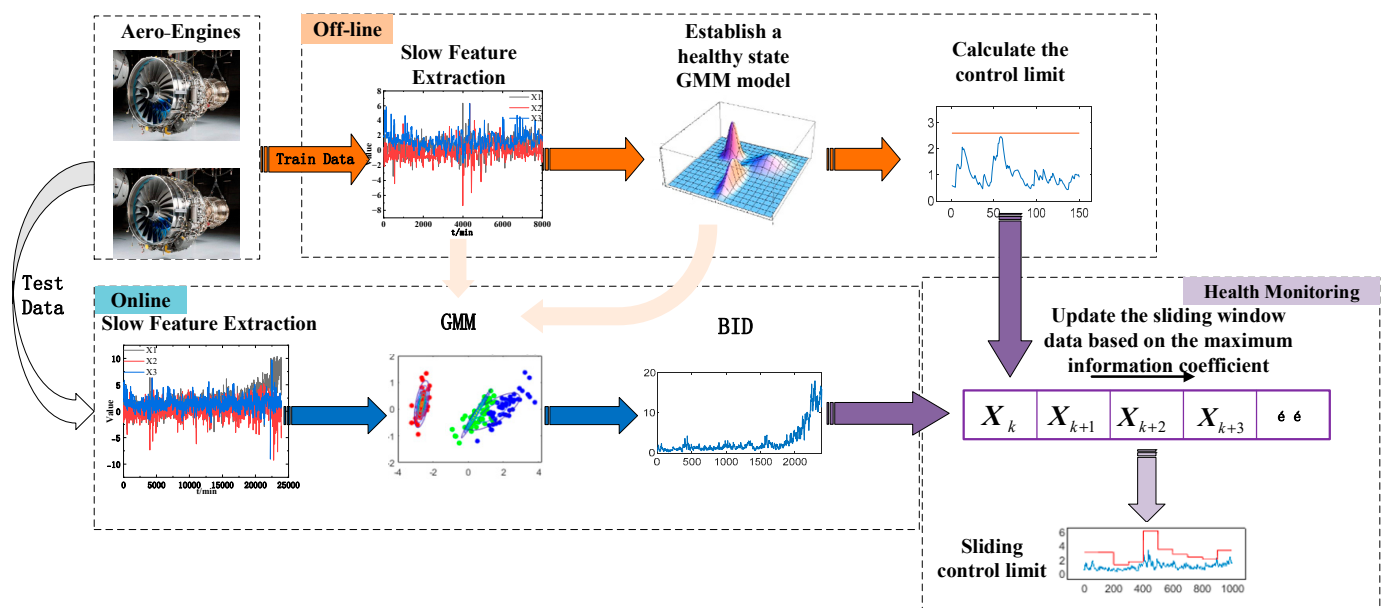


Figure 4. Flowchart of aero-engine dynamic health monitoring.

As seen in Figure 4, the operation of the aero-engine health monitoring method based on multi-feature fusion can be divided into offline and online stages. The specific steps are as follows:

(1) Offline stage

- A. Perform SFA on the training data and extract the slow features;
- B. Select the training data obtained under a healthy state to construct the GMM and obtain the parameters of the model;
- C. Calculate the BID value of the test data using the GMM parameters and describe the performance degradation process of the aero-engine. EWMA [38] is introduced to smooth and improve the sensitivity of BID to aero-engine degradation:

$$E_t = (1 - \alpha)E_{t-1} + \alpha BID_t \quad (24)$$

where E_t is the average of the first t data pieces; α is the smoothing coefficient, generally in the range from 0.05 to 0.25. The value of α is set to 0.2, reflecting the degradation trend quite well.

- D. Calculate the control limit of the training data.

(2) On-line stage

- A. Perform SFA on the training data and extract the slow features;
- B. Calculate the BID between the test data and the GMM of the healthy state;
- C. Perform sliding window processing on the BID data;
- D. Calculate the maximum information coefficient of adjacent window data, determine the forgetting factor, and update the sliding window data;
- E. Calculate the sliding control limit and set off the alarm when more than N consecutive outliers are detected.

5. Case Verification

We carried out a verification experiment on a set of data selected from the QAR data repository of the CFM56_7B engine used in the B737, which was provided by the China Academy of Civil Aviation Science and Technology, to demonstrate the effectiveness of the proposed health monitoring method for the aero-engine gas path. The verification dataset contains values of monitoring parameters of the aircraft engines acquired in the cruise state.

5.1. Case 1

5.1.1. Extraction of Slow Features

Case 1 is the flight data of two CFM56_7B engines used by the B737 recorded in 958 flights from 18 May 2019 to 19 May 2020 (defined as 958 cycles). The data recorded in the cruise stage of each flight were analyzed. The values of each parameter were averaged every 600 s to reflect the variation trend of each parameter, as shown in Figure 5.

As seen in Figure 5, the monitoring parameters of the left and right engines of the airplane exhibit no clear variation trend, so it is impossible to evaluate whether an engine is abnormal by merely examining the parameter variation curves of the left and right engines. Therefore, we used the SFA algorithm to extract the slow features of the parameters of the left and right engines and analyzed their variation patterns. The results are shown in Figure 6. X_1 to X_6 are the decomposed slow features sorted by the speed of change from fastest to slowest. The characteristics of the gas path extracted by slow characteristic analysis can reflect the changing process of the gas path to a certain extent.

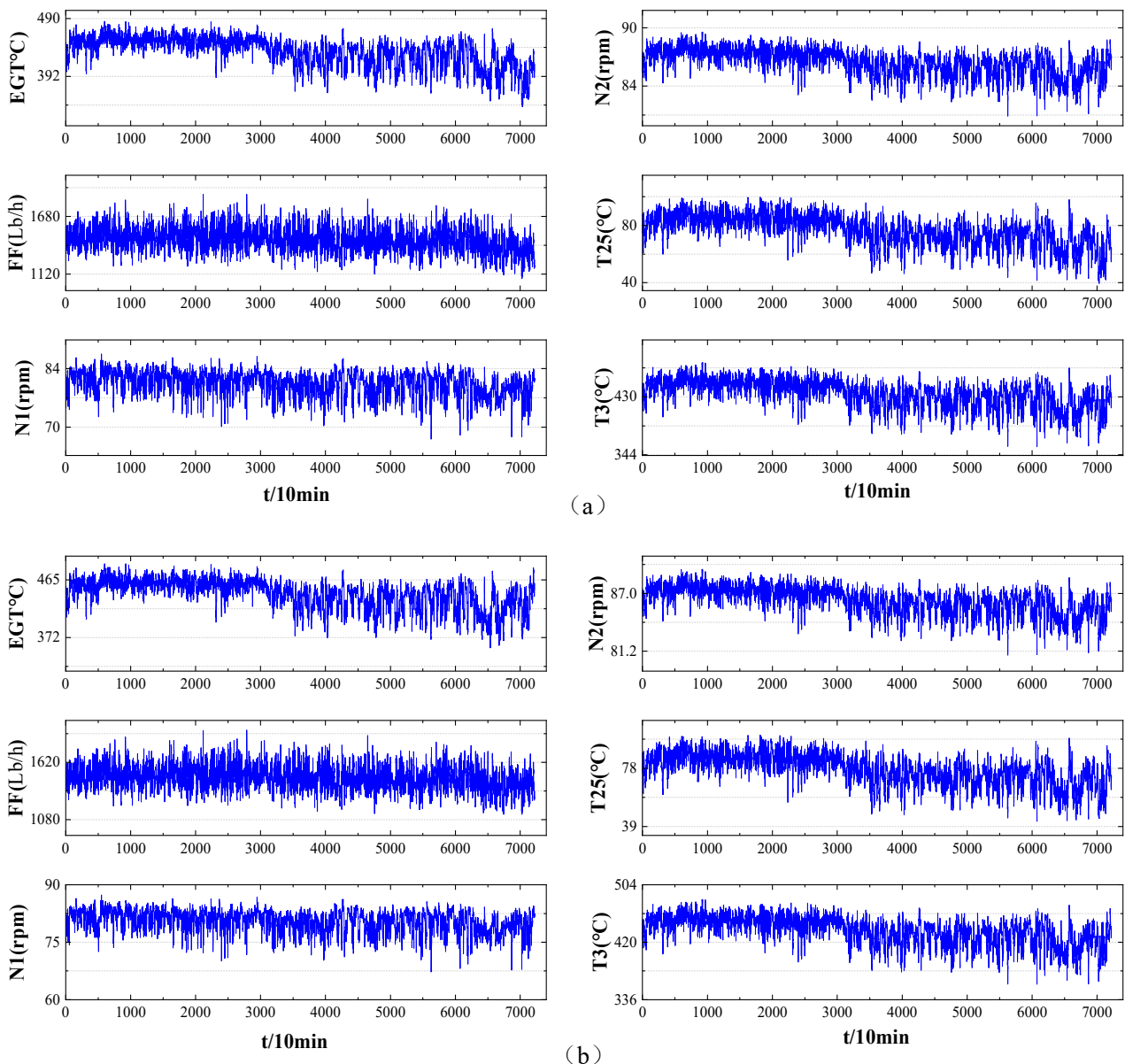


Figure 5. Variation curves of the parameters of two engines of an airplane. (a) Variation curves of the parameters of the left engine; (b) Variation curves of the parameters of the right engine.

As shown in Figure 6:

- (1) The decomposed features of six parameters of the two engines are stable in the first half of the observation period, indicating that extracting performance features of the engines using the SFA algorithm can mitigate the interference caused by the external environment or flight conditions.
- (2) All slow features of the six parameters of the left engine experienced an abrupt change to various extents near the end of the observation period, whereas such an abrupt change did not occur to the right engine. It can be evaluated that an anomaly occurred in the left engine at the time of the abrupt change. As opposed to employing the performance parameters of a single engine, extracting features using SFA can improve the sensitivity of identifying engine anomalies.
- (3) The performance features of the two engines extracted through SFA experienced significantly larger fluctuations in the second half of the observation period, increasing the number of false alarms during fault monitoring.

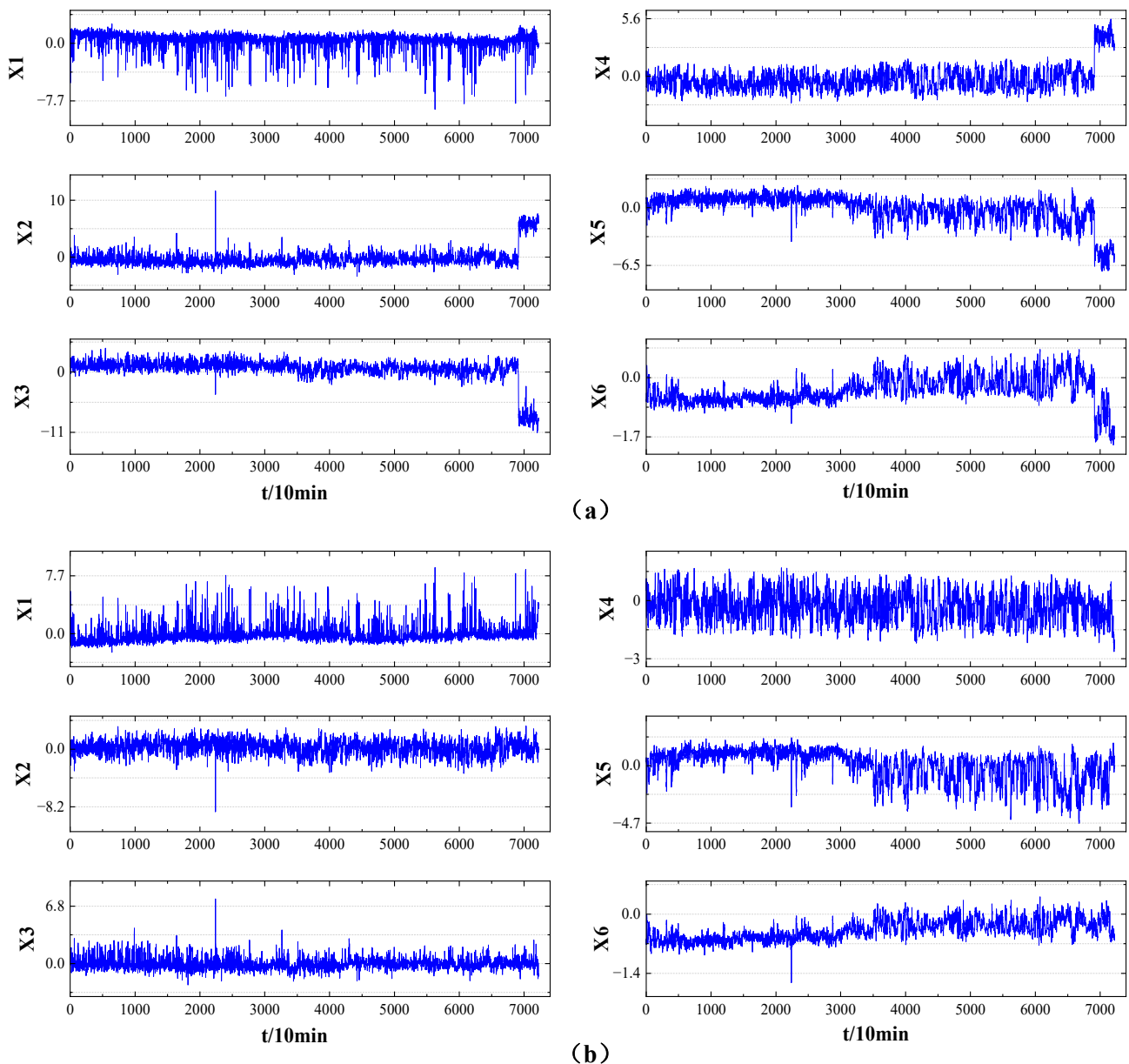


Figure 6. Slow features of two engines of an airplane. (a) Slow features of the left engine; (b) Slow features of the right engine.

5.1.2. Aero-Engine Dynamic Health Monitoring Based on SFA-GMM-BID

Based on the above analysis, the first 10% of data of the left and right engines in Case 1 were selected as the healthy-state data. After multiple experimental runs, the GMM with three Gaussian components accomplished the modeling of normal-state data very well. After the model training was completed, all the test data were input into the model as the test set to obtain the corresponding BID values. In the actual QAR record, the duration of each flight is about 2.5 h. Based on the test results and engineers' experience, the control limits will be updated every 10 flights, and exceeding the control limit for 1 consecutive hour (6 consecutive points exceeding the control limit) will be judged as an anomaly. In consequence, with the sliding window width and the sliding window step set to 150, the control limit was recursively updated to provide an early warning on the performance degradation of the aero-engine under study. The results are shown in Figure 7.

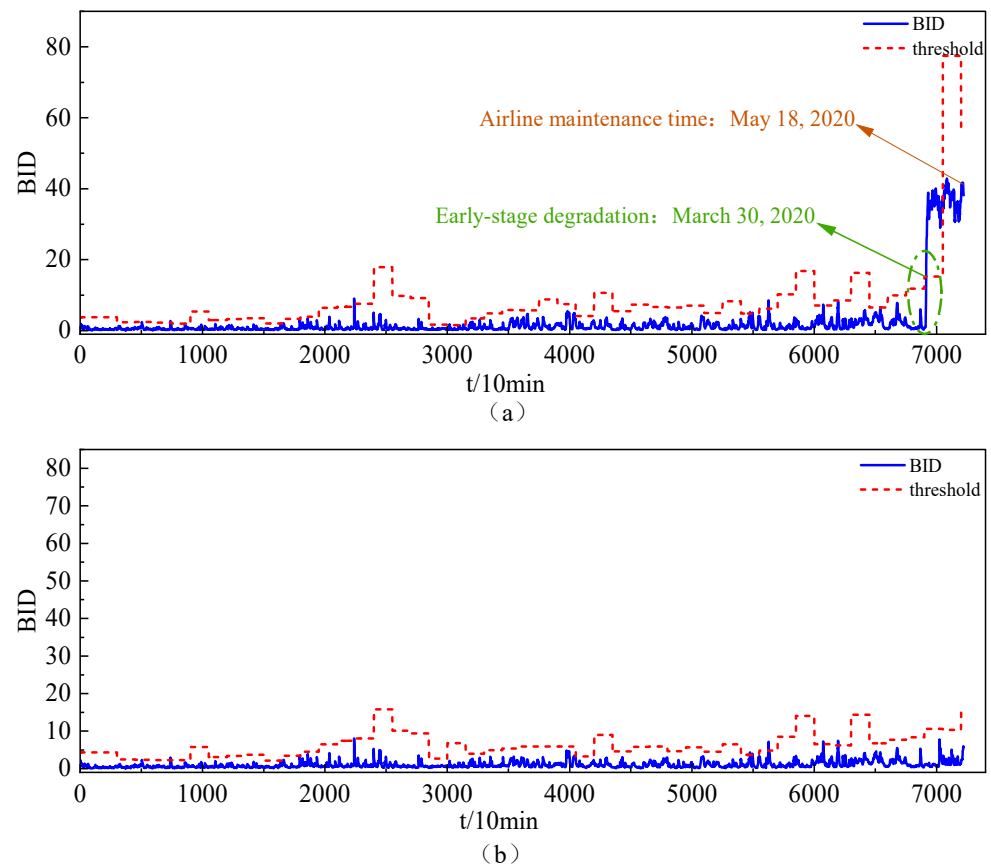


Figure 7. Dynamic health monitoring of two engines in case 1 based on SFA-GMM-BID. (a) Dynamic health monitoring of the left engine; (b) Dynamic health monitoring of the right engine.

The following conclusions can be drawn from Figure 7:

The BID value of the left engine remained stable in the first 919 cycles and then experienced an abrupt change in cycle 920 (the real time of this cycle is 30 March 2020). After a short period of abnormal fluctuation, the airline received an alarm in cycle 958, and the engine was repaired later (the corresponding real time is 18 May 2020). It was found during repair that the peeling caused the anomaly of the left engine off of the thermal barrier coating on the leading edge of the turbine blade (accompanied by signs of cracking). This demonstrates that the method proposed in this paper can identify anomalies in the aero-engine early, providing sufficient time for the maintenance personnel to make a sound maintenance plan for the engine. The BID value of the right engine did not exhibit any obvious abnormality before the airline received the alarm. During the inspection, no fault was found in the right engine, which also proved the effectiveness of the proposed method for anomaly monitoring.

5.2. Case 2

5.2.1. Extraction of Slow Features

Case 2 data represent the flight data of two CFM56_7B engines used by the B737 recorded in 319 flights from 7 February 2020 to 20 August 2020 (defined as 319 cycles). The data recorded in the cruise stage of each flight were analyzed. The values of each parameter were averaged every 600 s to reflect the variation trend of each parameter, as shown in Figure 8.

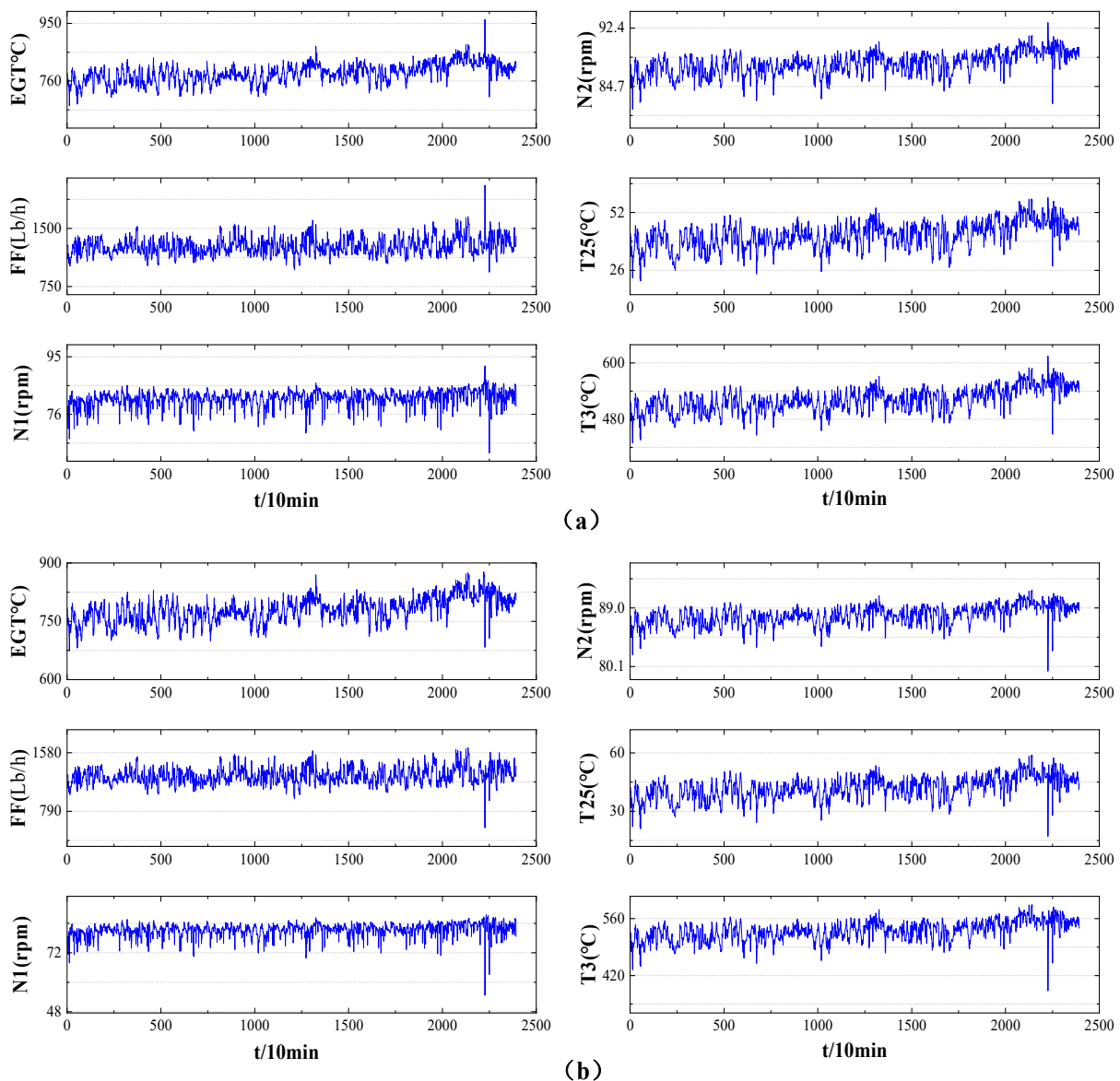


Figure 8. Variation curves of the parameters of two engines of an airplane. (a) Variation curves of the parameters of the left engine; (b) Variation curves of the parameters of the right engines.

According to Figure 8, the selected parameters do not exhibit a clear variation trend, so it is impossible to judge whether the engines are abnormal. Therefore, we used the SFA algorithm to extract the slow features of the parameters of the left and right engines and analyzed their variation patterns. The results are shown in Figure 9.

As shown in Figure 9, the decomposed slow features of the left engine are relatively stable in the first half of the observation period and do not exhibit any clear trend. By comparison, these features fluctuate considerably, with a clear upward/downward trend in the second half of the observation period. The decomposed features of the right engine are relatively stable. They only tend to increase fluctuation near the end of the observation period. Compared with the performance parameters of a single engine, the features extracted by KSFA can improve the sensitivity of engine anomaly recognition. However, since the trend is not very obvious and there are many spikes, the extracted features cannot be directly used for engine anomaly monitoring.

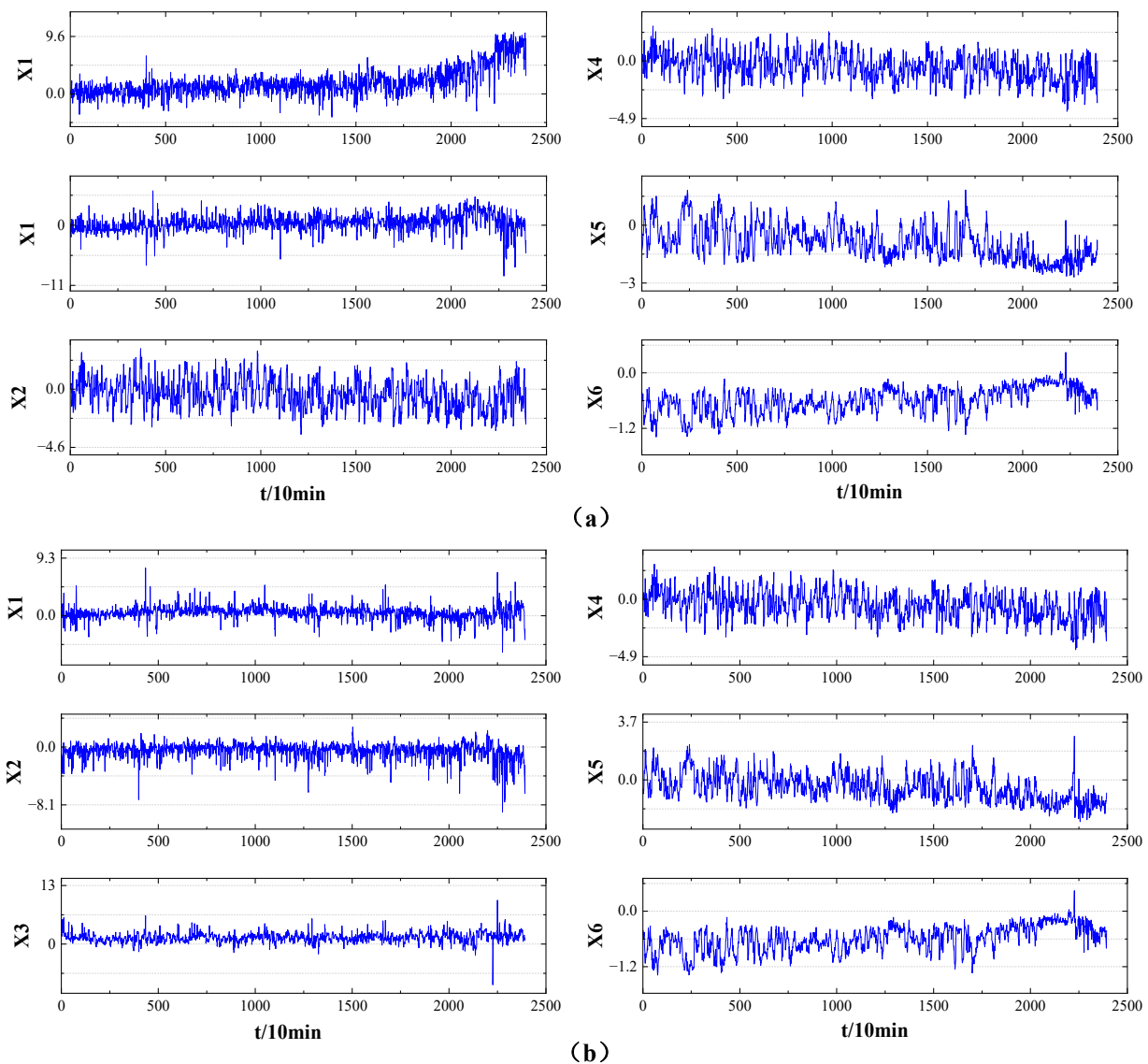


Figure 9. Slow features of the two engines in the same machine. (a) Slow features of the left engine; (b) Slow features of the right engine.

5.2.2. Dynamic Health Monitoring of Aero-Engine Based on SFA-GMM-BID

Based on the above analysis, we selected the first 10% of data of the left and right engines in Case 2 to serve as the healthy-state data. The GMM with three Gaussian components was used to model the healthy-state data and calculate the BID values. With both the sliding window width and the sliding window step set to 150, the control limit was recursively updated to provide early warning on the performance degradation of the engines. In this study, according to expert experience, exceeding the control limit for 1 consecutive hour (6 consecutive points exceeding the control limit) will be judged as an anomaly.

According to Figure 10, the left engine's BID exhibits a clear degradation trend. The engine showed a sign of early-stage degradation in cycle 263 (the corresponding time was 15 June 2020), and the degradation deteriorated sharply after cycle 263, which triggered an alarm. In cycle 319 (the corresponding time is 20 August 2020), the airline received an alarm from the aircraft, and repair was arranged for the engine. An inspection revealed that the engine's slow degradation of the radial bearing caused the fault. It can be seen that the method proposed in this paper can also detect hidden problems caused by the slow degradation of engine components at the early stage, which provides enough time for the

maintenance personnel to make a sound maintenance plan for the engine. Combining the two abnormal cases, it can be seen that the method proposed in this paper has a wider applicability, which can be better applied to all kinds of fault monitoring of aero-engine, and has great engineering application value.

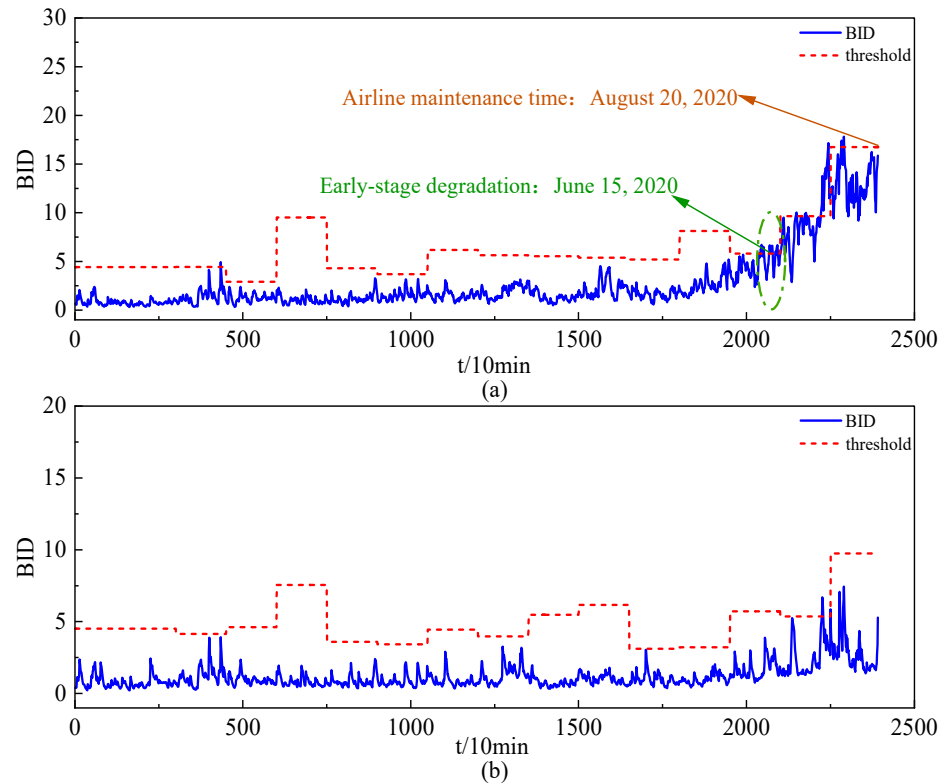


Figure 10. Dynamic health monitoring of two engines in case 2 based on SFA-GMM-BID. (a) Dynamic health monitoring of the left engine; (b) Dynamic health monitoring of the right engine.

6. Comparison and Analysis

6.1. Comparison with an Evaluation Method Based on PCA-GMM-BID

Principal component analysis (PCA) is often used in process monitoring as data feature extraction, which is often used for comparison with the proposed method [26]. To verify the effectiveness of the SFA-based data feature extraction, we used the process monitoring method based on PCA-GMM-BID to experiment on Cases 1 and 2. As shown in Figures 11 and 12, the process monitoring method based on PCA-GMM-BID cannot effectively describe the degradation process. In Case 1, the constructed BID experienced significantly larger fluctuations in the second half of the observation period, which also fails to indicate any experienced abrupt change near the end of the observation period. In Case 2, the constructed BID also failed to show an obvious degradation trend and only changed to a certain extent near the end of the observation period. Moreover, as shown in the two cases, PCA is difficult to accurately extract features that effectively represent the state of the engine. Therefore, the evaluation results of the left engine and the right engine are highly similar, resulting in difficulty to distinguish which engine failed. In normal condition monitoring, the state changes of left engine and right engine cannot be effectively monitored. Therefore, it is more difficult for this model to mine hidden useful information to characterize the normal and abnormal states and find early fault symptoms in time.

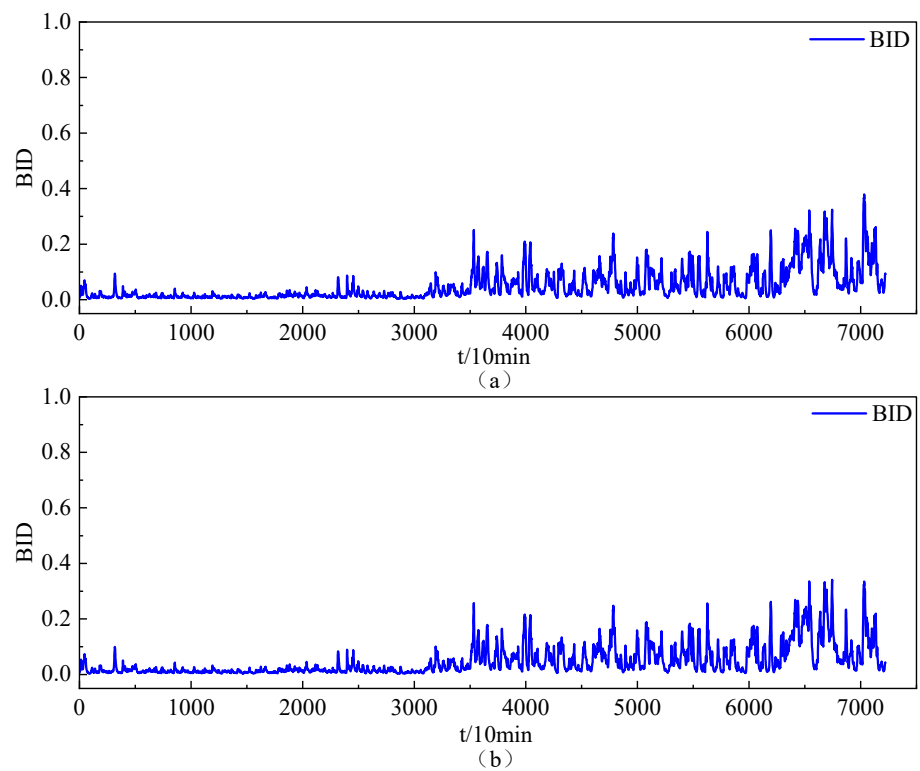


Figure 11. Process evaluation based on PCA-GMM-BID in Case 1. (a) Process evaluation of the left engine; (b) Process evaluation of the right engine.

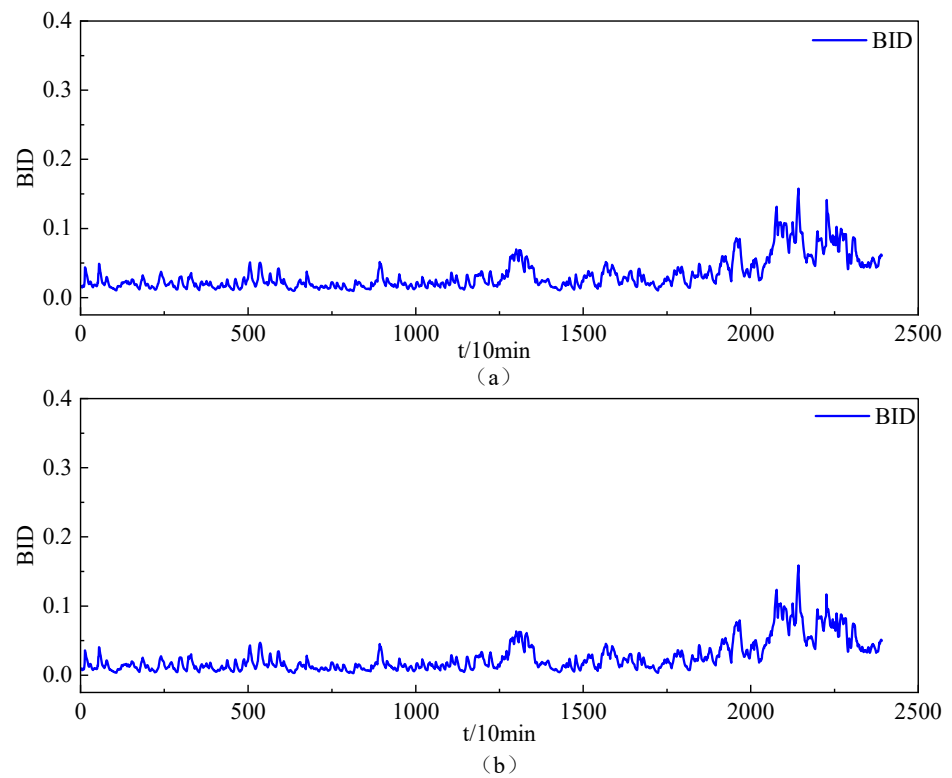


Figure 12. Process evaluation based on PCA-GMM-BID in Case 2. (a) Process evaluation of the left engine; (b) Process evaluation of the right engine.

6.2. Comparison with an SFA-Based Process Monitoring Method

To verify the effectiveness of the constructed BID, we used the process monitoring method based on SFA to experiment on Cases 1 and 2, in which the statistical quantities used were T^2 and SPE. It can be seen from Figures 13 and 14 that T^2 can effectively describe the degradation process in Case 1. In Case 2, however, T^2 fluctuates in a larger range without indicating any clear degradation trend, which is not conducive to fault monitoring. SPE fails to indicate any clear trend in Cases 1 and 2, and local abnormal values occur randomly, showing that this statistical quantity is unsuitable for detecting aero-engines anomalies. Intermittent false alarms are hardly valuable for airlines to make maintenance plans.

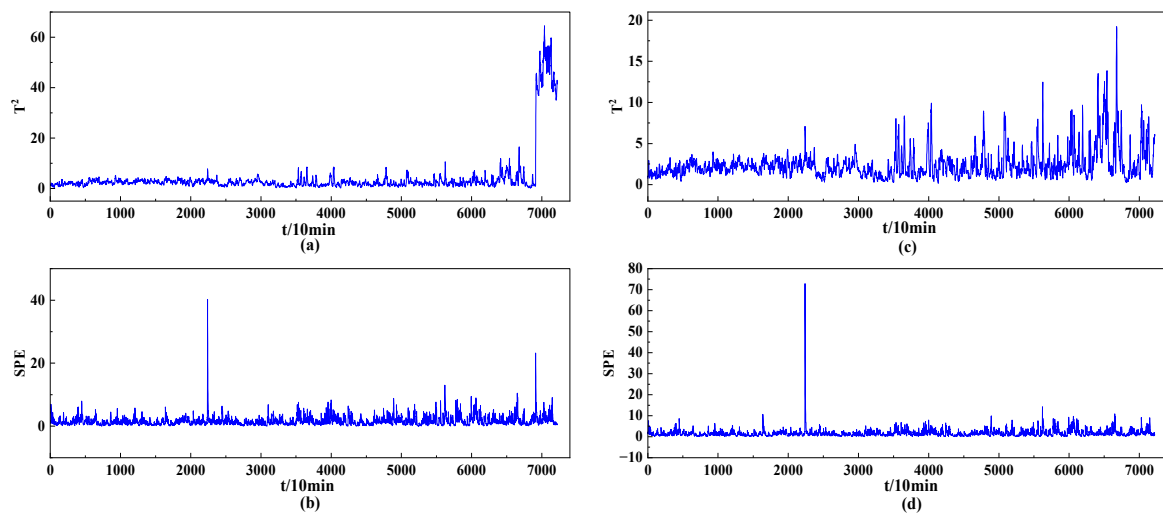


Figure 13. Process monitoring based on SFA in Case 1. (a) Process monitoring of the left engine based on T^2 ; (b) Process monitoring of the left engine based on SPE; (c) Process monitoring of the right engine based on T^2 ; (d) Process monitoring of the right engine based on SPE.

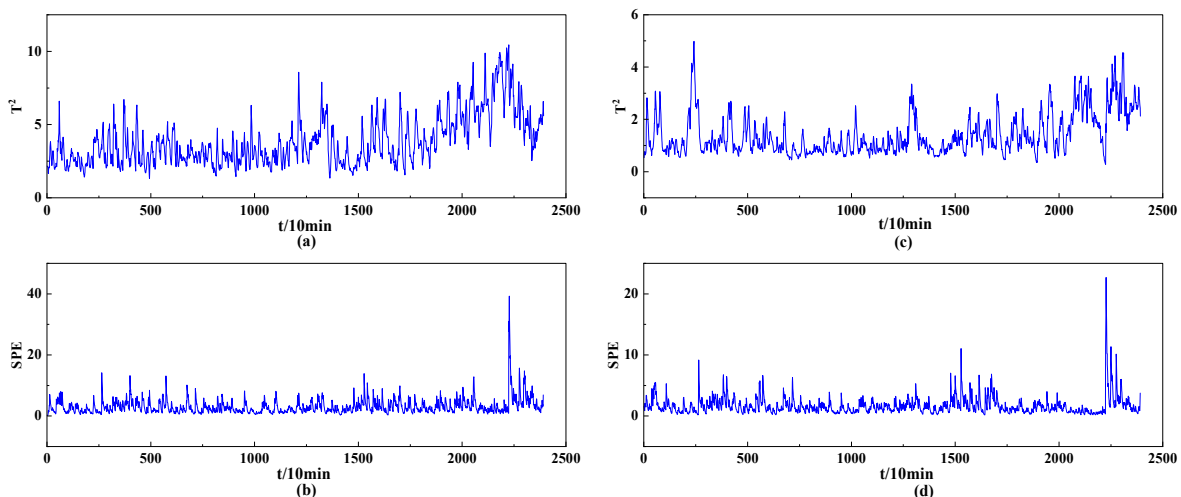


Figure 14. Process monitoring based on SFA in Case 2. (a) Process monitoring of the left engine based on T^2 ; (b) Process monitoring of the left engine based on SPE; (c) Process monitoring of the right engine based on T^2 ; (d) Process monitoring of the right engine based on SPE.

6.3. Comparison with an SVDD-Based Evaluation Method

To verify the effectiveness of the constructed BID, we used the state evaluation method based on SVDD to experiment on Cases 1 and 2. SVDD is a distance-based state evaluation method, which is widely used in fault diagnosis and health monitoring [41]. We selected

the left and right engines' first 10% of data as the healthy-state data, used the Gaussian kernel function as the kernel function, and set the penalty factor to 0.3. The SVDD model was trained using the healthy-state data, obtaining a hypersphere. With this hypersphere serving as the benchmark, the kernel distance between the test data and the hypersphere was used as the performance evaluation parameter. The evaluation results based on SFA-SVDD are shown in Figures 15 and 16. It can be observed that:

- (1) In Case 2, the constructed distance indicator (DI) is effective in detecting the degradation trend of the left engine;
- (2) In Case 1, DI fluctuates considerably in the second half of the observation period, which can cause the frequent occurrence of false alarms during normal state monitoring, indicating that DI is unsuitable for fault detection.

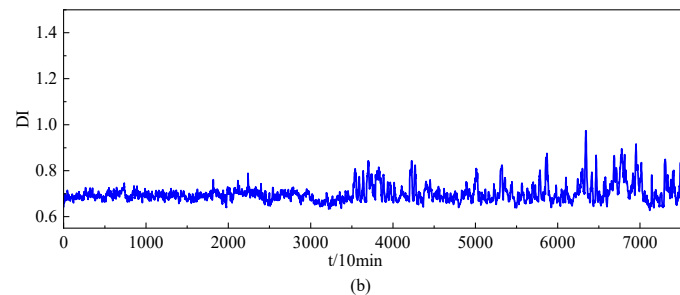
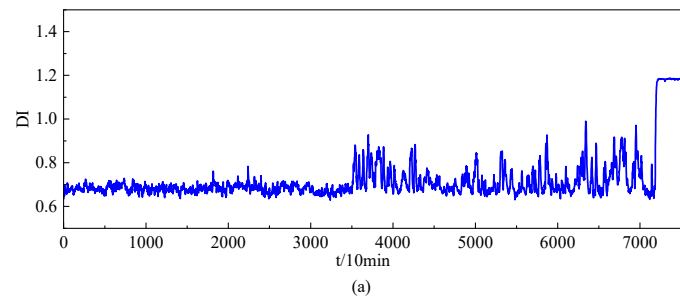


Figure 15. Process evaluation based on SFA-SVDD in Case 1. (a) Process evaluation of the left engine; (b) Process evaluation of the right engine.

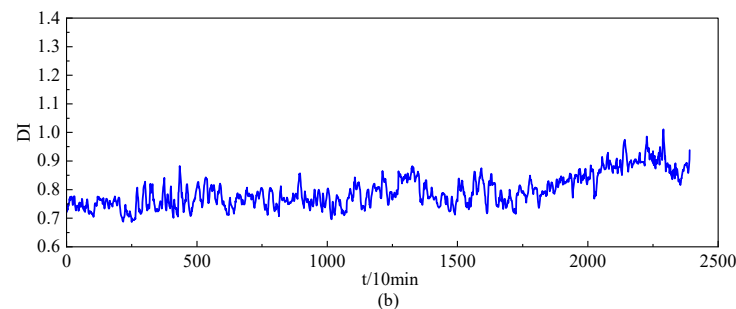
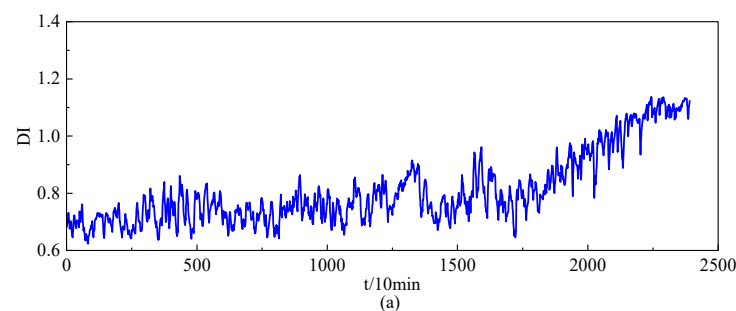


Figure 16. Process evaluation based on SFA-SVDD in Case 2. (a) Process evaluation of the left engine; (b) Process evaluation of the right engine.

6.4. Comparison between Adaptive Threshold and Conventional Threshold

We calculated the control limits of the training data of various events and used them as the control limits for subsequent monitoring to verify the effectiveness of the constructed adaptive threshold. The results are shown in Figures 17 and 18. Because the conventional threshold cannot be updated recursively, this limitation can cause false alarms, as demonstrated in the results of the two cases: In Case 1, many BID values exceeded the control limit, triggering a continuous false alarm. In Case 2, there were also some false alarms. By comparison, using the control limit that can be updated recursively based on the maximum information coefficient can effectively avoid this problem. In the aero-engine dynamic anomaly monitoring based on the model constructed in this paper, false alarms appear in both Case 1 and Case 2, and can effectively monitor the engine abnormal state.

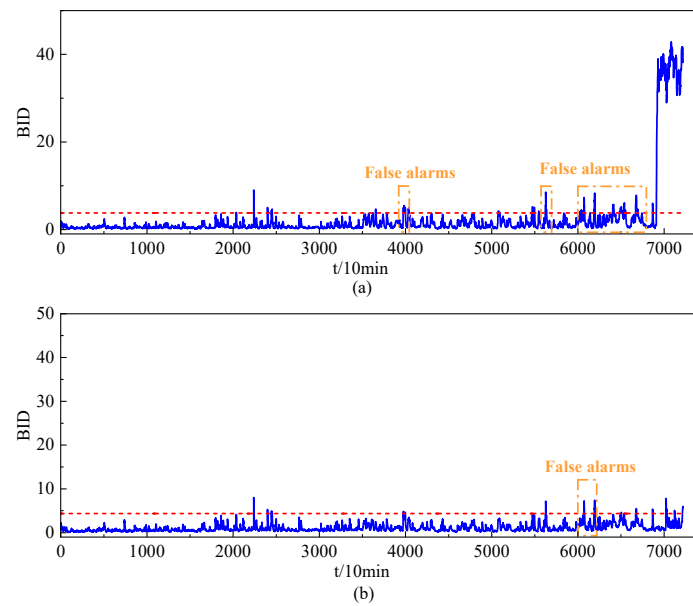


Figure 17. Health monitoring based on a conventional threshold in Case 1. (a) Health monitoring of the left engine; (b) Health monitoring of the right engine.

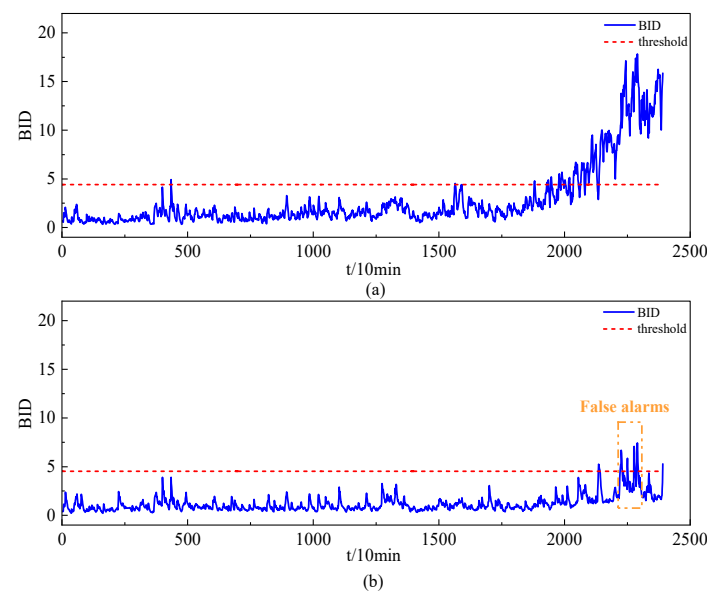


Figure 18. Health monitoring based on a conventional threshold in Case 2. (a) Health monitoring of the left engine; (b) Health monitoring of the right engine.

7. Conclusions

This paper proposes an aero-engine dynamic health monitoring method based on SFA-GMM-BID. The experimental results show the following:

- (1) The approach of extracting the effective features reflecting the slow variation of the gas-path state using the SFA method suits the slow time-varying characteristics of aero-engines, which is conducive to improving the performance of health monitoring.
- (2) The BID-based GMM proposed in this paper combines multiple features to characterize the degradation degree of the aero-engine. Compared with the SVDD evaluation method and indicators like T2 and SPE, the proposed method is more suitable for monitoring various types of faults of aero-engines and, therefore, has higher value in real-world applications.
- (3) The adoption of the dynamic threshold based on the maximum information coefficient ensures that the contribution of the old samples to the new sample threshold is considered when updating the threshold using a sliding window. The use of a dynamic threshold can effectively reduce the occurrence of false alarms, which is superior to the conventional fixed threshold.

Author Contributions: Y.Z.: Conceptualization, Methodology, Validation, Writing—review and editing. D.L.: Software, Investigation, Project administration, Writing—original draft. Y.L.: Validation, Writing—review and editing. T.Z.: Validation, Writing—review and editing. J.C.: Data curation, Formal analysis. H.Z.: Funding acquisition, Formal analysis. All authors have read and agreed to the published version of the manuscript.

Funding: This research is supported by the Joint Funds of the National Natural Science Foundation of China (U1933202).

Data Availability Statement: Not applicable.

Conflicts of Interest: The authors declare no conflict of interest.

References

1. Tian, J.; Yang, M.F. Research on trajectory tracking and body attitude control of autonomous ground vehicle based on differential steering. *PLoS ONE* **2023**, *18*, e0273255. [[CrossRef](#)] [[PubMed](#)]
2. Yao, J.L.; Ge, Z. Path-Tracking Control Strategy of Unmanned Vehicle Based on DDPG Algorithm. *Sensors* **2022**, *22*, 7881. [[CrossRef](#)] [[PubMed](#)]
3. Zhou, W.L.; Zheng, Y.P.; Pan, Z.J.; Lu, Q. Review on the Battery Model and SOC Estimation Method. *Processes* **2021**, *9*, 1685. [[CrossRef](#)]
4. Li, D.X.; Xu, B.; Tian, J.; Ma, Z.S. Energy Management Strategy for Fuel Cell and Battery Hybrid Vehicle Based on Fuzzy Logic. *Processes* **2020**, *8*, 882. [[CrossRef](#)]
5. Zhou, W.L.; Lu, Q.; Zheng, Y.P. Review on the Selection of Health Indicator for Lithium Ion Batteries. *Machines* **2022**, *10*, 512. [[CrossRef](#)]
6. Lin, Y.; Xiao, M.H.; Liu, H.J.; Li, Z.L.; Zhou, S.; Xu, X.M.; Wang, D.C. Gear fault diagnosis based on CS-improved variational mode decomposition and probabilistic neural network. *Measurement* **2022**, *192*, 110913. [[CrossRef](#)]
7. Sun, S.S.; Zhang, X.Z.; Wan, M.S.; Gong, X.L.; Xu, X.M. Study of Quenched Crankshaft High-Cycle Bending Fatigue Based on a Local Sub Model and the Theory of Multi-Axial Fatigue. *Metals* **2022**, *12*, 913. [[CrossRef](#)]
8. Wang, A.C.; Zhang, Y.; Zuo, H.F. Assessing the Performance Degradation of Lithium-Ion Batteries Using an Approach Based on Fusion of Multiple Feature Parameters. *Math. Probl. Eng.* **2019**, *2019*, 3091071. [[CrossRef](#)]
9. Yuan, Y.; Ding, S.; Liu, X.; Pan, Q. Hybrid Diagnosis System for Aeroengine Sensor and Actuator Faults. *J. Aerosp. Eng.* **2020**, *33*, 04019108. [[CrossRef](#)]
10. Zhang, K.; Lin, B.; Chen, J.; Wu, X.; Lu, C.; Zheng, D.; Tian, L. Aero-Engine Surge Fault Diagnosis Using Deep Neural Network. *Comput. Syst. Sci. Eng.* **2022**, *42*, 351–360. [[CrossRef](#)]
11. Zhou, X.; Fu, X.; Zhao, M.; Zhong, S. Regression model for civil aero-engine gas path parameter deviation based on deep domain-adaptation with Res-BP neural network. *Chin. J. Aeronaut.* **2021**, *34*, 79–90. [[CrossRef](#)]
12. Sun, H.; Fu, X.; Zhong, S. A Weakly Supervised Gas-Path Anomaly Detection Method for Civil Aero-Engines Based on Mapping Relationship Mining of Gas-Path Parameters and Improved Density Peak Clustering. *Sensors* **2021**, *21*, 4526. [[CrossRef](#)] [[PubMed](#)]

13. Mao, P.; Lin, Y.; Xue, S.; Zhang, B. Remaining Useful Life Estimation of Aircraft Engines Using Differentiable Architecture Search. *Mathematics* **2022**, *10*, 352. [[CrossRef](#)]
14. Li, B.; Zhao, Y.-P. Group reduced kernel extreme learning machine for fault diagnosis of aircraft engine. *Eng. Appl. Artif. Intell.* **2020**, *96*, 103968. [[CrossRef](#)]
15. Fentaye, A.D.; Zaccaria, V.; Kyprianidis, K. Aircraft Engine Performance Monitoring and Diagnostics Based on Deep Convolutional Neural Networks. *Machines* **2021**, *9*, 337. [[CrossRef](#)]
16. Zhou, L.; Wang, H.; Xu, S. Aero-engine gas path system health assessment based on depth digital twin. *Eng. Fail. Anal.* **2022**, *142*, 106790. [[CrossRef](#)]
17. Jin, P.; Lu, F.; Huang, J.; Kong, X.; Fan, M. Life cycle gas path performance monitoring with control loop parameters uncertainty for aeroengine. *Aerosp. Sci. Technol.* **2021**, *115*, 106775. [[CrossRef](#)]
18. Chang, X.; Huang, J.; Lu, F.; Sun, H. Gas-Path Health Estimation for an Aircraft Engine Based on a Sliding Mode Observer. *Energies* **2016**, *9*, 598. [[CrossRef](#)]
19. Smart, E.; Brown, D.; Denman, J. Combining multiple classifiers to quantitatively rank the impact of abnormalities in flight data. *Appl. Soft Comput.* **2012**, *12*, 2583–2592. [[CrossRef](#)]
20. Melnyk, I.; Banerjee, A.; Matthews, B.; Oza, N.; Assoc Comp, M. Semi-Markov Switching Vector Autoregressive Model-Based Anomaly Detection in Aviation Systems. In Proceedings of the 22nd ACM SIGKDD International Conference on Knowledge Discovery and Data Mining (KDD), San Francisco, CA, USA, 13–17 August 2016; pp. 1065–1074.
21. Jiang, W.; Xu, Y.; Chen, Z.; Zhang, N.; Xue, X.; Zhou, J. Measurement of health evolution tendency for aircraft engine using a data-driven method based on multi-scale series reconstruction and adaptive hybrid model. *Measurement* **2022**, *199*, 111502. [[CrossRef](#)]
22. Wang, H.; Jiang, W.; Deng, X.; Geng, J. A new method for fault detection of aero-engine based on isolation forest. *Measurement* **2021**, *185*, 110064. [[CrossRef](#)]
23. Lu, F.; Jiang, J.; Huang, J.; Qiu, X. An Iterative Reduced KPCA Hidden Markov Model for Gas Turbine Performance Fault Diagnosis. *Energies* **2018**, *11*, 1807. [[CrossRef](#)]
24. Nie, L.; Xu, S.; Zhang, L.; Yin, Y.; Dong, Z.; Zhou, X. Remaining Useful Life Prediction of Aeroengines Based on Multi-Head Attention Mechanism. *Machines* **2022**, *10*, 552. [[CrossRef](#)]
25. Wang, H.; Wang, X.; Wang, Z. Performance assessment method of dynamic process based on SFA-GPR. *J. Process Control* **2022**, *111*, 27–34. [[CrossRef](#)]
26. Cheng, C.; Liu, M.; Chen, H.; Xie, P.; Zhou, Y. Slow feature analysis-aided detection and diagnosis of incipient faults for running gear systems of high-speed trains. *ISA Trans.* **2022**, *125*, 415–425. [[CrossRef](#)]
27. Amirkhani, S.; Chaibakhsh, A.; Ghaffari, A. Nonlinear robust fault diagnosis of power plant gas turbine using Monte Carlo-based adaptive threshold approach. *ISA Trans.* **2020**, *100*, 171–184. [[CrossRef](#)]
28. Zhao, W.; Guo, Y.; Sun, H. Research on an Adaptive Threshold Setting Method for Aero-Engine Fault Detection Based on KDE-EWMA. *J. Aerosp. Eng.* **2022**, *35*, 04022087. [[CrossRef](#)]
29. Ammiche, M.; Kouadri, A.; Bensmail, A. A Modified Moving Window dynamic PCA with Fuzzy Logic Filter and application to fault detection. *Chemom. Intell. Lab. Syst.* **2018**, *177*, 100–113. [[CrossRef](#)]
30. Yang, F.; Cui, Y.; Wu, F.; Zhang, R. Fault Monitoring of Chemical Process Based on Sliding Window Wavelet DenoisingGLPP. *Processes* **2021**, *9*, 86. [[CrossRef](#)]
31. Shi, J.; Guo, H.; Chen, D. Parameter identification method for lithium-ion batteries based on recursive least square with sliding window difference forgetting factor. *J. Energy Storage* **2021**, *44*, 103485. [[CrossRef](#)]
32. Song, B.; Shi, H.; Tan, S.; Tao, Y. Serial correlated-uncorrelated concurrent space method for process monitoring. *J. Process Control* **2021**, *105*, 292–301. [[CrossRef](#)]
33. Xie, X.; Lin, L.; Zhong, S. Process Takagi-Sugeno model: A novel approach for handling continuous input and output functions and its application to time series prediction. *Knowl.-Based Syst.* **2014**, *63*, 46–58. [[CrossRef](#)]
34. Luo, H.; Zhong, S. Gas Turbine Engine Gas Path Anomaly Detection Using Deep Learning with Gaussian Distribution. In Proceedings of the 2017 Prognostics and System Health Management Conference (PHM-Harbin), Harbin, China, 9–12 July 2017; pp. 312–317.
35. Wiskott, L.; Berkes, P.; Franzius, M.; Sprekeler, H.; Wilbert, N. Slow Feature Analysis. *J. Mach. Learn. Res.* **2011**, *6*, 5282. [[CrossRef](#)]
36. Zhao, X.; Zhang, C.; Yang, B.; Li, P. Adaptive knot placement using a GMM-based continuous optimization algorithm in B-spline curve approximation. *Comput.-Aided Des.* **2011**, *43*, 598–604. [[CrossRef](#)]
37. Dempster, A.P.; Laird, N.M.; Rubin, D.B. Maximum Likelihood from Incomplete Data via the EM Algorithm. *J. R. Stat. Society. Ser. B (Methodol.)* **1977**, *39*, 1–12.
38. Yu, J. Bearing performance degradation assessment using locality preserving projections and Gaussian mixture models. *Mech. Syst. Signal Process.* **2011**, *25*, 2573–2588. [[CrossRef](#)]
39. Zhang, Y.; Wang, A.; Zuo, H. Roller Bearing Performance Degradation Assessment Based on Fusion of Multiple Features of Electrostatic Sensors. *Sensors* **2019**, *19*, 824. [[CrossRef](#)]

40. Reshef, D.N.; Reshef, Y.A.; Finucane, H.K.; Grossman, S.R.; McVean, G.; Turnbaugh, P.J.; Lander, E.S.; Mitzenmacher, M.; Sabeti, P.C. Detecting Novel Associations in Large Data Sets. *Science* **2011**, *334*, 1518–1524. [[CrossRef](#)] [[PubMed](#)]
41. Zhao, Y.-P.; Xie, Y.-L.; Ye, Z.-F. A new dynamic radius SVDD for fault detection of aircraft engine. *Eng. Appl. Artif. Intell.* **2021**, *100*, 104177. [[CrossRef](#)]

Disclaimer/Publisher's Note: The statements, opinions and data contained in all publications are solely those of the individual author(s) and contributor(s) and not of MDPI and/or the editor(s). MDPI and/or the editor(s) disclaim responsibility for any injury to people or property resulting from any ideas, methods, instructions or products referred to in the content.